STRATIGRAPHY OF THE NORTHEAST SYRTIS MAJOR MARS 2020 LANDING SITE AND THE EJECTA OF JEZERO CRATER, MARS. M. S. Bramble[1], J. F. Mustard[1], C. I. Fassett[2], and T. A. Goudge[3], [1]Department of Earth, Environmental, and Planetary Sciences, Brown University, Providence, RI, USA (michael_bramble@brown.edu), [2]NASA Marshall Space Flight Center, Huntsville, AL, USA, [3]Jackson School of Geosciences, The University of Texas at Austin, Austin, TX, USA.

Introduction: Northeast Syrtis Major (NE Syrtis), Mars is a region with diverse alteration mineralogy suggesting the presence of four distinct aqueous environments in a stratigraphy bookended by the formation of the Isidis basin and the emplacement of the Syrtis Major volcanic province [1,2]. The candidate NE Syrtis landing ellipse for the Mars 2020 rover is situated at approximately one crater radius beyond the rim of Jezero crater. Therefore, the ellipse is likely located near or within the area that was affected by emplacement of Jezero's continuous ejecta, meaning excavated material 10s to ~100 m thick may have been locally deposited [3–5]. Because of Jezero's Noachian age, however, its ejecta may have been entirely removed from the stratigraphic record at NE Syrtis via erosion. The question of whether remnants of Jezero's ejecta persist has significant implications for the local erosional history, the stratigraphy at the landing site, and the origin of the materials now exposed at the surface.

Of particular interest are the Large Linear Features (LLF) and the basement unit of [2]. The LLF are light-toned linear structures 10s to 100s of meters wide and 1000s of meters long that are hypothesized to be mineralized fracture zones, material infilling troughs, and/or breccia or igneous dykes [2,6]. They qualitatively appear radial to Jezero, and may offer clues at the landscape evolution of the region. The basement unit of the region displays various morphologies and erosional states, and, being the stratigraphically lowest unit identified, these outcrops would be the most likely to contain, or be stratigraphically below, remnant Jezero ejecta. Therefore, in this analysis we focus on the morphology and topography of the LLF and basement unit to search for evidence of Jezero ejecta.

Methods: To confirm the qualitative observation of the LLF being radial to Jezero, the orientations of the LLF were surveyed in the SW quadrant of Jezero between one and two radii from the center. LLF were mapped if they were identified as LLF in [2], or if a feature matching LLF characteristics was observed >500 m in length. The analysis was performed with Context Camera (CTX) [7] mosaics at 1:10,000 scale, and with only one mapped line per feature. The orientations of the LLF were calculated by taking the azimuth of a line though a feature's start and end points, and the results were rotated to be within 0 and 180 ° due to the arbitrariness of start versus end point.

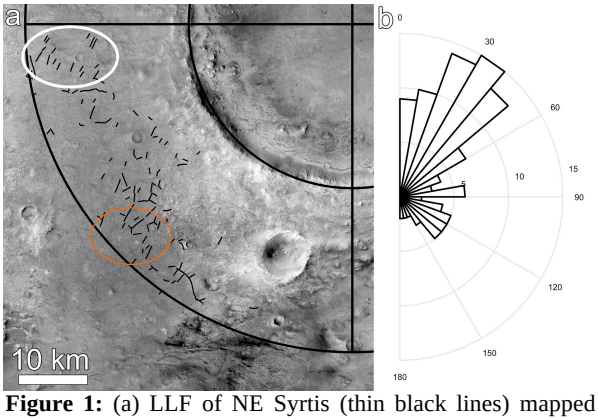

Figure 1: (a) LLF of NE Syrtis (thin black lines) mapped within one crater radius of the SW rim of Jezero crater. The NE Syrtis Mars 2020 ellipse is shown in red and the features discussed in the text in the white ellipse, both overlain on a mosaic of CTX imagery. (b) The 111 LLF mapped in this quadrant show a modest preferred orientation to the NE-SW.

To search for ejecta remnants in NE Syrtis, radial profiles were taken using a Mars Orbiter Laser Altimeter (MOLA) [8] elevation map and digital elevation models (DEMs) produced using CTX stereo pairs and the NASA Ames Stereo Pipeline [9–11]. These profiles were sampled at 100 m or 5 m increments for the MOLA or CTX data, respectively. These profiles were then compared to profiles produced in a similar manner of an unnamed crater of comparable radius in Isidis Planitia (10 °N, 94 °E).

Results: In total, 111 LLF were mapped in the SW quadrant of Jezero crater between one and two crater radii (**Figure 1a**). The calculated orientations show a modest preference for NE-SW, approximately towards the center of Jezero crater (**Figure 1b**).

Radial profiles show significant deviation between NE Syrtis and the Isidis Planitia crater (**Figure 2**). MOLA profiles taken at 5 ° anticlockwise increments show steepening slopes with radial distance through NE Syrtis. This steepening slope is mostly the result of a regional slope towards the S. Other deviations are caused by the E-W valley through NE Syrtis, an erosional depression outside the SW rim of Jezero, and the Depression region and Large Crustal Mounds of [2]. When compared to the Isidis Planitia crater, these profiles also show that the NE Syrtis region is significantly high-standing in comparison (**Figure 2d**). In other words, the present surface surrounding Jezero lies significantly above the profile of the analog crater's ejecta using their rims as a reference. The re-

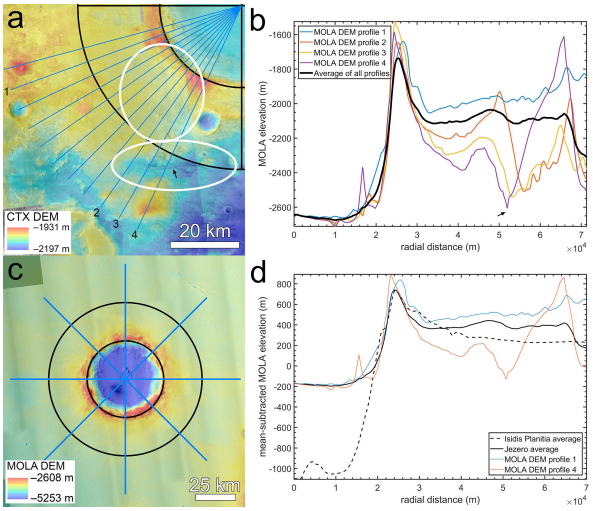

Figure 2: (a) Radial profiles through NE Syrtis from the center of Jezero crater at 5° increments. Features discussed in the text (white ellipses) and the E-W valley (arrow) are shown. Mosaic of CTX-derived DEMs overlain on a CTX mosaic. (b) MOLA-derived profiles corresponding to the numbered profiles in (a), plus an average of all 11 profiles, showing the radial topographic characteristics at NE Syrtis. (c) Radial profiles of 8 cardinal directions of an unnamed crater in Isidis Planitia. MOLA topography overlain on a mosaic of CTX imagery. (d) MOLA-derived profiles from (b) with the average of the profiles in (c) in the dashed line.

gional slope complicates this, but the regional trend and large mounds are commonly high-standing and erosional features low-standing relative to the average Isidis Planitia profile.

CTX profiles taken with small degrees of separation (to circumvent major deviations from regional slope) show that high-standing, eroded basement mounds near NE Syrtis are commonly ~50 m tall, and up to ~150 m tall (**Figure 3**).

Discussion: The LLF are orientated roughly radial to Jezero crater at NE Syrtis. This observation could support the formation of these features by infilling of fractures or radial structures formed by eroding Jezero ejecta, but this hypothesis is complicated by LLF in the northernmost part of this quadrant showing SW orientations, where they should be fully W. Therefore, this may be due to aeolian erosion preferentially favoring ridge formation in the observed orientation from a dominant wind direction (e.g., as yardangs) rather than any ejecta fabric. The other three quadrants within one crater radius from Jezero's rim reveal a paucity of LLF, though a few radial troughs are observed.

Outside the SW rim of Jezero, basement mounds 50–100 m in height are observed, and, if they were taken to be the original ejecta surface, then the erosion to produce these mounds would be less than the expected thickness of an ejecta blanket (100–200 m). Nearer and within the NE Syrtis ellipse, mounds of similar height are observed, and here the mounds would suggest erosion through the ejecta (~50 m).

Conclusions: LLF at NE Syrtis are approximately radial to Jezero crater, suggesting they could be related to the emplacement and erosion of Jezero ejecta. However, their orientations are perhaps better explained by regional aeolian erosion and infilling. The surface of NE Syrtis spans the topography expected of the ejecta of Jezero, with the average elevation greater, and some erosional features lower, than the average of a younger crater of similar diameter. The basement mounds at NE Syrtis show that erosion has removed material equal to or greater than estimated ejecta thicknesses prior to the emplacement of the olivine-rich unit. An updated geological history of NE Syrtis based on these findings would include the formation of Jezero, deposition both inside and around Jezero, erosion forming the NE-SW trending troughs, then deposition of the circum-Isidis olivine-rich unit. Therefore, it appears highly probable that the pre-existing target materials, materials excavated by the formation of Jezero crater, and later deposited materials compose the basement at NE Syrtis.

Acknowledgements: We utilized data products produced by Jay Dickson and the Bruce Murray Laboratory for Planetary Visualization.

References: [1] Ehlmann B. L. and Mustard J. F. (2012) *GRL*, 39, L11202. [2] Bramble M. S. et al. (2017) *Icarus*, 293, 66–93. [3] Melosh H. J. (2011) *Cambridge University Press* (9780511977848). [4] McGetchin T. R. et al. (1973) *EPSL*, 20, 226-236. [5] Sturm S. et al. (2016) *JGR*, 121, 1026–1053. [6] Thomas et al. (2017) *GRL*, 44, 6579–6588. [7] Malin M. C. et al. (2007) *JGR*, 112, E05S04. [8] Smith D. E. et al. (2001) *JGR*, 106, 23689–23722. [9] Broxton M. J. and Edwards L. J. (2008) *LPS XXXIX*, Abstract #2419. [10] Moratto Z. M. et al. (2010) *LPS XLI*, Abstract #2364. [11] Shean, D. E. et al. (2016) *ISPRS J. Photogramm. Remote Sens.*, 116, 101–117.

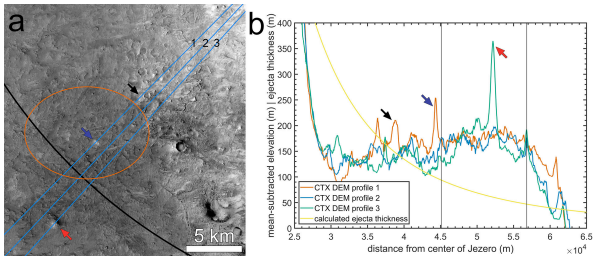

Figure 3: (a) CTX mosaic of NE Syrtis depicting high-standing basement mounds. Three numbered CTX radial profiles are shown with arrows depicting notable mounds seen in (b). (b) Mean-subtracted profiles derived from a mosaic of CTX DEMs depicting high-standing basement mounds. A calculated ejecta thickness using a radial power law [4] and the total thickness of MC9 from [5] is plotted for comparison with the basement mound heights. Vertical black lines show the near and far points of the ellipse.